Electromagnetics-Based Channel Model of Reconfigurable Intelligent Surfaces

Franek, Ondrej

Published in:
2023 17th European Conference on Antennas and Propagation (EuCAP)

DOI (link to publication from Publisher):
10.23919/EuCAP57121.2023.10133029

Publication date:
2023

Document Version
Accepted author manuscript, peer reviewed version

Electromagnetics-Based Channel Model of Reconfigurable Intelligent Surfaces

Ondřej Franek*
*Antennas, Propagation, and Millimeter-Wave Systems Section,
Department of Electronic Systems,
Aalborg University, Denmark,
of@es.aau.dk

***Abstract*—Motivated by recently growing interest in reconfigurable intelligent surfaces (RIS), we introduce a channel model of communication between two arbitrarily positioned end devices assisted by a RIS, where all three devices are characterized using off-the-shelf electromagnetic simulation software. The communication between the devices is assumed to occur via planar electromagnetic waves. This approach correctly represents the electromagnetic coupling between the RIS elements, and also allows the user to choose additional complex weights for path loss between the devices. The user is given a scattering or impedance matrix that exposes all ports of the involved devices, including the RIS element ports, which can be used to optimize the RIS performance for various goals.**

***Index Terms*—Reconfigurable intelligent surfaces, electromagnetics, propagation.**

I. Introduction

With the advent of the 6th generation (6G) wireless networks, novel concepts that would address the increased performance requirements have emerged. One of these is the concept of modification of propagation environments using reconfigurable intelligent surfaces (RIS) [1]. RIS are large arrays of passive scattering elements whose scattering properties can be controlled by electronic circuits. Strategically distributed RIS in the environment, with sufficient sizes and proper settings of their elements, have the potential to improve coverage and therefore reliability of wireless networks, and, at the same time, reduce unintended electromagnetic field exposure to persons that are not involved in the communication [2].

To evaluate the performance improvements added by RIS, we need accurate and realistic models of RIS that could be incorporated in propagation models of radio environment. This is currently an active research area, although only few models of RIS-assisted communication that would reflect the electromagnetic behavior of RIS have been proposed. In [3], the communication model is based on path loss model with known transmitting and receiving properties of the RIS elements, although no mention is made about the effect of mutual coupling. Another path loss model, this time based on the vector generalization of Green's theorem, is presented in [4]. In [5], the authors present a phase model of RIS that is made more realistic by assuming phase-dependent amplitude variation of the element reflective properties. In [6], the RIS model is based on impedance matrix taking into account also the coupling

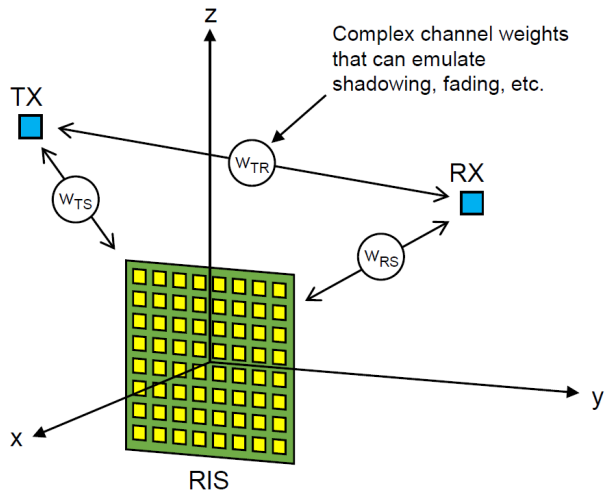

Fig. 1. Overview of the proposed electromagnetics-based model: The RIS is positioned at the origin of coordinates facing the x-direction, TX and RX represent the wireless communication participants at arbitrary positions; All 3 devices are characterized by electromagnetic simulations and communication between them is established via electromagnetic plane waves with arbitrary complex weights on each segment.

between the elements. In [7], the proposed RIS model is electromagnetically compliant and formulated as end-to-end, accounting for mutual coupling between the RIS elements and for arbitrary amplitude and phase response. In [8], the physics-based model of RIS is based on partitioning the unit cells of RIS into tiles and treating these as anomalous reflectors. In [9], the RIS is modeled analytically using equivalent circuit obtained from full-wave simulations. Another RIS model is based on an analytical representation of the periodic surface using transmission line circuit approach and homogenized impedance [10]. Finally in [11], the communication model of RIS is derived using scattering parameter network analysis.

All previously proposed approaches use some kind of approximations of the RIS to avoid using apparently costly electromagnetic simulations, which, however, at the same time leads to those approaches being questionable in terms of generality and accuracy. In this work, we decided to take the straightforward approach and to design a channel model that uses full-wave simulations to characterize the RIS in its

entirety, i.e. including inter-element coupling and arbitrary incidence angles, without resorting to too many approximations. Apart from the fact that the RIS itself is modeled numerically with finite numerical errors and precision, the only approximation of the proposed model is the assumption that the communication between all pairs of devices in the system occurs via planar electromagnetic waves. The decision for this assumption resulted in the following four advantages:

1) Electromagnetic characterization of all involved devices can be carried out in any simulation software that supports plane wave excitation and near-to-far-field transformation, i.e. in wide range of commercially available products.
2) The number of simulations that need to be performed can be limited to reasonable levels, as each device is illuminated from directions given by only two spherical coordinates θ and ϕ, as opposed to exposure from all points in space.
3) Linking the three devices together can be performed swiftly by using scattering matrix formalism instead of more general Green's functions.
4) The paths between the three devices can easily be assigned arbitrary complex weights to emulate channel properties different from those of free space, such as fading or complete blockage.

On the other hand, the plane wave assumption should not be seen as a severe limitation, since the far-field regime has long been used to characterize antennas via their radiation patterns.

The model is intended mainly for higher level communication studies involving end devices placed at arbitrary positions with respect to the RIS. The scattering matrices that characterize all three devices are precomputed and stored in a file. The user provides information about the positions of the two communicating devices, denoted in the following text as transmitter (TX) and receiver (RX), although their roles can be arbitrary. In addition, the user provides complex weights for the path loss between all pairs of devices. The result of the model is the scattering ($\mathbf{S}$) or impedance ($\mathbf{Z}$) matrix of the entire system, where the ports of both TX and RX, as well all ports of the passive elements of RIS are exposed. This enables the user to optimize the loads attached to the ports of the RIS, with various goals, for example the best coverage at selected positions.

II. System Model

An overview of the proposed electromagnetics-based model is shown in Fig. 1. The RIS is positioned at the origin of spatial coordinates $(0, 0, 0)$ with its face oriented in the x-direction. The TX and RX represent the participants in the RIS-assisted wireless communication, and may have arbitrary positions in space, provided that the distances between the devices d ensure far-field conditions [12],

$$d > 2D^2/\lambda \tag{1}$$

where D is the largest physical dimension of either of the two involved devices, and λ is the wavelength.

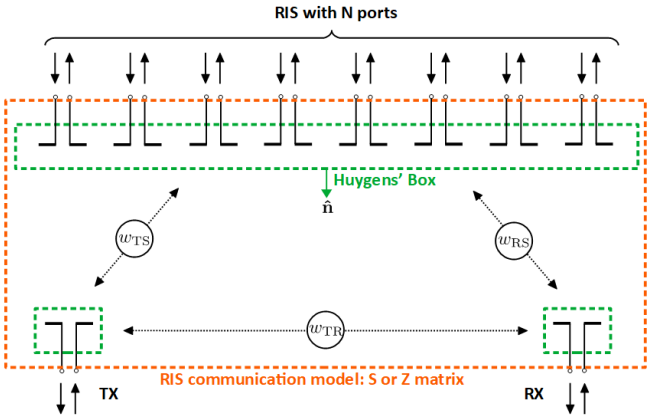

Fig. 2. Schematic view of the underlying electromagnetic model: TX, RX, and RIS are enclosed in Huygens' boxes (green dashed rectangles) that allow plane wave communication between each of these 3 devices with arbitrary channel weights w_{TR}, w_{TS}, w_{RS}; the user is given an S- or Z-matrix of the entire system (red dashed rectangle) that exposes only the ports of the 3 devices.

The far-field condition (1) is not a "hard" limit, but for lower distances the accuracy of this model quickly deteriorates. The reason for this limitation is twofold. First, if the far-field condition (1) is satisfied, we can assume TX, RX, and RIS to be irradiated by plane waves (or good approximations thereof), which reduces the amount of electromagnetic simulations that need to be performed to characterize each device, so that this approach can be considered practical. Second, the plane wave assumption allows to easily incorporate arbitrary complex weights w_{TR}, w_{TS}, w_{RS}, between the devices (T stands for TX, R for RX, and S for the RIS), that can emulate for example fading or blockage using the usual path-loss formalism.

III. Electromagnetic Model

The electromagnetic principle of the RIS channel model is depicted in Fig. 2. The problem of obtaining the communication channel is divided into three parts following the three involved devices: TX, RX, and RIS. For each of these devices, a set of electromagnetic simulations is performed to characterize it in terms of incoming and outgoing power waves at each port and incoming and outgoing plane waves in free space. For the latter, a Huygens' box [13] is formed, entirely enclosing each device (green dashed rectangles in Fig. 2) and used for a) illuminating the device with plane waves and b) recording of the electromagnetic fields radiated or scattered from the device. The recorded fields are then developed using the near-to-far-field transformation into radiation or scattering patterns that express the magnitude and phase of the produced plane wave at the far-field distance.

At this point, the model does not yet know the positions of TX and RX with respect to RIS, as this information will only be provided by the user of the model. Therefore, each device must be electromagnetically characterized in advance, assuming arbitrary positions of the other devices, which could easily lead to excessive number of simulations needed. To keep the

approach practical, we chose to illuminate the devices by plane waves (implying far-field conditions (1)) from finite number of spatial directions. In particular, the spatial directions are distributed in a rectangular grid of two spherical coordinates θ and ϕ with predefined angular steps $\Delta\theta$ and $\Delta\phi$. If we denote the sizes of the grid in the θ and ϕ dimensions as $N_\theta = \pi/\Delta\theta$ and $N_\phi = 2\pi/\Delta\phi$, respectively, then the total number of simulations for each polarization will generally be $N = (N_\theta - 1)N_\phi + 2$ (as each "pole" of the spherical coordinate system needs to be counted only once). However, if the device is symmetrical, as is often the case with RIS in the form of planar arrays, we can take advantage of available geometrical and functional symmetries and reduce the number of simulations accordingly.

Each device is characterized by three distinct matrices: 1) the port scattering matrix $\mathbf{S}^{[M\times M]}$, which carries information about coupling between the M ports of the device, 2) the radiation matrix $\mathbf{H}^{[N\times M]}$, which carries information about the radiation (and, by reciprocity, reception) properties of the device in N directions for each port, and 3) the plane wave scattering matrix $\mathbf{\Sigma}^{[N\times N]}$, which carries information about scattering from the device in N directions when illuminated by a plane wave from each of the N directions. In the following, let us assume only single polarization with all the devices. If the simulation engine provides complex values for the radiated E-field of the chosen polarization at 1 m distance in the matrix $\mathbf{E}_{\mathrm{rad}}^{[N\times M]}$, then the radiation matrix can be calculated

$$\mathbf{H} = \mathbf{E}_{\mathrm{rad}} \frac{\lambda \mathrm{e}^{\mathrm{j}k}}{\mathrm{j}\sqrt{\eta_0}} \tag{2}$$

where $k = 2\pi/\lambda$ is the wavenumber, η_0 is the free space wave impedance, and j is the imaginary unit. Similarly, the scattered E-fields at 1 m distance normalized to an incident plane wave of 1 V/m provided in the matrix $\mathbf{E}_{\mathrm{scat}}^{[N\times N]}$ can be converted to the plane wave scattering matrix

$$\mathbf{\Sigma} = \mathbf{E}_{\mathrm{scat}} \frac{\lambda \mathrm{e}^{\mathrm{j}k}}{\mathrm{j}} \tag{3}$$

The three matrices $\mathbf{S}$, $\mathbf{H}$, and $\mathbf{\Sigma}$ are then stored in a file.

The final step in obtaining the model is to assemble the three devices into one system, by coupling all pairs of devices with their plane wave ports (dotted arrows in Fig. 2). This step is only possible after the user provides the positions of the TX and RX. First, the precomputed matrices are loaded from the file, and reduced to include only relevant directions, so only those columns corresponding to the directions toward the other devices are retained in $\mathbf{H}$ and the rows and columns with these same indices are retained in $\mathbf{\Sigma}$. If the directions do not exactly coincide with the data grid, interpolation may be employed. All matrices for TX, RX, and RIS are gathered together into system matrices

$$\mathbf{S}_{\mathrm{sys}} = \mathrm{blkdiag}(\mathbf{S}_{\mathrm{TX}}, \mathbf{S}_{\mathrm{RX}}, \mathbf{S}_{\mathrm{RIS}}) \tag{4}$$

$$\mathbf{H}_{\mathrm{sys}} = \mathrm{blkdiag}(\mathbf{H}_{\mathrm{TX}}, \mathbf{H}_{\mathrm{RX}}, \mathbf{H}_{\mathrm{RIS}}) \tag{5}$$

$$\mathbf{\Sigma}_{\mathrm{sys}} = \mathrm{blkdiag}(\mathbf{\Sigma}_{\mathrm{TX}}, \mathbf{\Sigma}_{\mathrm{RX}}, \mathbf{\Sigma}_{\mathrm{RIS}}) \tag{6}$$

where $\mathrm{blkdiag}()$ is a shorthand for block diagonal matrix. The three devices are then linked together using free space propagation terms [14] multiplied by the user-provided complex channel weights

$$\mathbf{F} = \mathrm{diag}\left(w_{\mathrm{TR}} \frac{\mathrm{j}\mathrm{e}^{-\mathrm{j}kr_{\mathrm{TR}}}}{\lambda r_{\mathrm{TR}}}, w_{\mathrm{TS}} \frac{\mathrm{j}\mathrm{e}^{-\mathrm{j}kr_{\mathrm{TS}}}}{\lambda r_{\mathrm{TS}}}, w_{\mathrm{RS}} \frac{\mathrm{j}\mathrm{e}^{-\mathrm{j}kr_{\mathrm{RS}}}}{\lambda r_{\mathrm{RS}}} \right) \tag{7}$$

where r_{TR}, r_{TS}, r_{RS} are the geometric distances between the three devices. The path loss matrix $\mathbf{F}$ is instrumental in creating the connector matrix

$$\mathbf{C} = \begin{bmatrix} \mathbf{0} & \mathbf{F} \\ \mathbf{F} & \mathbf{0} \end{bmatrix} \tag{8}$$

that is finally used to eliminate the internal plane wave ports to give the user the total scattering matrix $\mathbf{S}_{\mathrm{tot}}$ of the entire system (red dashed rectangle in Fig. 2) with only the physical ports (dual arrows in Fig. 2) of the TX, RX, and RIS exposed,

$$\mathbf{S}_{\mathrm{tot}} = \mathbf{S}_{\mathrm{sys}} + \mathbf{H}_{\mathrm{sys}}^{\mathrm{T}} \left(\mathbf{C}^{-1} - \mathbf{\Sigma}_{\mathrm{sys}} \right)^{-1} \mathbf{H}_{\mathrm{sys}} \tag{9}$$

If needed, the scattering matrix can be converted to impedance matrix assuming Z_0 is the characteristic impedance of all the ports

$$\mathbf{Z}_{\mathrm{tot}} = Z_0 \left(\mathbf{I} + \mathbf{S}_{\mathrm{tot}} \right) \left(\mathbf{I} - \mathbf{S}_{\mathrm{tot}} \right)^{-1} \tag{10}$$

where $\mathbf{I}$ is the identity matrix of the same size as $\mathbf{S}_{\mathrm{tot}}$.

IV. Implementation

Since the proposed model uses plane waves to link the three communication participants, TX, RX, and RIS, together, the simulations can be performed in off-the-shelf commercial software for electromagnetic simulations of antennas, as they usually offer both the plane wave excitation and near-to-far-field transformation. For our implementation, we chose CST Microwave Studio [15] as the simulation engine, and Matlab [16] for the wrapper function that performs the linking and the interface to the user. The syntax of the Matlab function is

```
M = ris_matrix( type, filename, ...
                x_TX, y_TX, z_TX, ...
                x_RX, y_RX, z_RX, ...
                w_TR, w_TS, w_RS )
```

where `M` is the resulting matrix that can be the S- or Z-matrix of the entire model (denoted by red dashed rectangle in Fig. 2) depending on the argument `type` being `'S'` or `'Z'`, respectively. Argument `filename` specifies the file in which the precomputed simulation data are stored, `x_TX, y_TX, z_TX` and `x_RX, y_RX, z_RX` are the spatial Cartesian coordinates of the TX and RX, respectively, and finally `w_TR, w_TS, w_RS` are the arbitrary complex weights w_{TR}, w_{TS}, w_{RS}, respectively.

TABLE I
MAXIMUM ERROR OF THE COMPUTED IMPEDANCE MATRIX ELEMENTS

RIS size	magnitude error [%]	phase error [°]
2×2	0.52	3
4×4	0.94	3
8×8	1.2	2
16×16	1.4	2

V. VALIDATION

The model has been validated against a full-wave simulation of the scenario described in [7] and [17] at frequency 28 GHz. The RIS is an $P \times P$ planar array centered at coordinates $(0, 0, 0)$ facing the x direction. The RIS elements are distributed in a rectangular grid with spacing λ/P, making the electrical size of the RIS approx. $\lambda \times \lambda$. The TX and RX, as well as all the elements of the RIS array, are z-oriented short dipoles with length $\lambda/32$ and radius $\lambda/500$. The TX is positioned at coordinates $(5, -5, 3)$ and RX at $(5, 5, 1)$, measured in meters.

The errors of the resulting $(P + 2) \times (P + 2)$ impedance matrix elements between the full-wave simulation and the proposed model are listed in Table I. The maximum error is less than 1.4 % in magnitude ($<$0.12 dB) and less than 3° in phase. When assuming only the line-of-sight path between TX and RX, then the error is $<$0.14 % ($<$0.02 dB) in magnitude and $<3°$ in phase.

VI. CONCLUSION

We have introduced a RIS-assisted channel model of communication between two end devices, where all three devices are accurately characterized by their electromagnetic behavior. The main advantage of this model is that it assumes all radiated or scattered waves to be planar at the distances involved, which allows for using commercial off-the-shelf simulation software to characterize the electromagnetic behavior of the three devices, and for their relatively straightforward linking using scattering matrix formalism. It is worth mentioning that this feature is also the main limitation of the approach, as the model cannot be used when the communication devices are in the near-field of the RIS, and such situation can indeed occur for large RIS at lower frequency bands. Moreover, the preparation phase of the model involves large number of simulations of the RIS, with many ports, which may be very time-consuming.

On the other hand, since the RIS is always simulated as one unit, the inter-element coupling between all the RIS ports is correctly modeled. In addition, it is possible to supply information about the path loss between the devices in the form of complex weight coefficients, so that it is possible to study fading or blockage scenarios as well. The model can be wrapped in another layer of abstraction, if that is desired, with given known loads at the RIS ports, so that only the ports of the TX and RX are exposed to the user. We are now working towards application of this model to a realistic scenario of indoor coverage enhancement.

ACKNOWLEDGMENT

This work has been supported by the EU Horizon 2020 project RISE-6G.

REFERENCES

[1] E. Basar, M. Di Renzo, J. De Rosny, M. Debbah, M.-S. Alouini, and R. Zhang, "Wireless communications through reconfigurable intelligent surfaces," *IEEE Access*, vol. 7, pp. 116 753–116 773, 2019.

[2] E. C. Strinati, G. C. Alexandropoulos, V. Sciancalepore, M. Di Renzo, H. Wymeersch, D.-T. Phan-Huy, M. Crozzoli, R. d'Errico, E. De Carvalho, P. Popovski *et al.*, "Wireless environment as a service enabled by reconfigurable intelligent surfaces: The RISE-6G perspective," in *2021 Joint European Conference on Networks and Communications & 6G Summit (EuCNC/6G Summit)*. IEEE, 2021, pp. 562–567.

[3] W. Tang, M. Z. Chen, X. Chen, J. Y. Dai, Y. Han, M. Di Renzo, Y. Zeng, S. Jin, Q. Cheng, and T. J. Cui, "Wireless communications with reconfigurable intelligent surface: Path loss modeling and experimental measurement," *IEEE Transactions on Wireless Communications*, vol. 20, no. 1, pp. 421–439, 2020.

[4] F. H. Danufane, M. Di Renzo, J. De Rosny, and S. Tretyakov, "On the path-loss of reconfigurable intelligent surfaces: An approach based on Green's theorem applied to vector fields," *IEEE Transactions on Communications*, vol. 69, no. 8, pp. 5573–5592, 2021.

[5] S. Abeywickrama, R. Zhang, Q. Wu, and C. Yuen, "Intelligent reflecting surface: Practical phase shift model and beamforming optimization," *IEEE Transactions on Communications*, vol. 68, no. 9, pp. 5849–5863, 2020.

[6] R. J. Williams, E. De Carvalho, and T. L. Marzetta, "A communication model for large intelligent surfaces," in *2020 IEEE International Conference on Communications Workshops (ICC Workshops)*. IEEE, 2020, pp. 1–6.

[7] G. Gradoni and M. Di Renzo, "End-to-end mutual coupling aware communication model for reconfigurable intelligent surfaces: An electromagnetic-compliant approach based on mutual impedances," *IEEE Wireless Communications Letters*, vol. 10, no. 5, pp. 938–942, 2021.

[8] M. Najafi, V. Jamali, R. Schober, and H. V. Poor, "Physics-based modeling and scalable optimization of large intelligent reflecting surfaces," *IEEE Transactions on Communications*, vol. 69, no. 4, pp. 2673–2691, 2020.

[9] D. Hanna, M. S. Melo, F. Shan, and F. Capolino, "A versatile polynomial model for reflection by a reflective intelligent surface with varactors," in *2022 IEEE International Symposium on Antennas and Propagation and USNC-URSI Radio Science Meeting (AP-S/URSI)*. IEEE, 2022, pp. 679–680.

[10] F. Costa and M. Borgese, "Electromagnetic model of reflective intelligent surfaces," *IEEE Open Journal of the Communications Society*, vol. 2, pp. 1577–1589, 2021.

[11] S. Shen, B. Clerckx, and R. Murch, "Modeling and architecture design of reconfigurable intelligent surfaces using scattering parameter network analysis," *IEEE Transactions on Wireless Communications*, vol. 21, no. 2, pp. 1229–1243, 2021.

[12] C. A. Balanis, *Antenna Theory: Analysis and Design*. John Wiley & Sons, 2015.

[13] ——, *Advanced Engineering Electromagnetics*. John Wiley & Sons, 2012.

[14] O. Franek, "Phasor alternatives to Friis' transmission equation," *IEEE Antennas and Wireless Propagation Letters*, vol. 17, no. 1, pp. 90–93, 2017.

[15] "CST Studio Suite," https://www.3ds.com/products-services/simulia/products/cst-studio-suite/, accessed: 2022-10-12.

[16] "Matlab," https://se.mathworks.com/products/matlab.html, accessed: 2022-10-12.

[17] X. Qian and M. Di Renzo, "Mutual coupling and unit cell aware optimization for reconfigurable intelligent surfaces," *IEEE Wireless Communications Letters*, vol. 10, no. 6, pp. 1183–1187, 2021.